Available online at www.sciencedirect.com
ScienceDirect
Applied Catalysis B: Environmental 80 (2008) 296–305
APPLIED CATALYSIS B: ENVIRONMENTAL
www.elsevier.com/locate/apcatb

C_2H_2 oxidation by plasma/TiO_2 combination: Influence of the porosity, and photocatalytic mechanisms under plasma exposure

O. Guaitella [a,*], F. Thevenet [a,b], E. Puzenat [b], C. Guillard [b], A. Rousseau [a,*]

[a] *LPTP, Ecole Polytechnique, CNRS UMR 7648, 91 128 Palaiseau, France*
[b] *LACE, CNRS, Université Claude Bernard LYON 1, 69622 Villeurbanne Cedex, France*

Received 21 September 2007; received in revised form 19 November 2007; accepted 24 November 2007
Available online 5 December 2007

Abstract

Plasma/catalyst combination is an active solution to reach high conversion rates at low energetic cost. TiO_2 is one of the catalysts frequently used in dielectric barrier discharges. Plasma/TiO_2 synergy was already exhibited but the mechanisms still have to be understood. This work distinguishes three main effects involved in the synergy: (a) effect of catalyst on the injected power, (b) the effect of porosity on C_2H_2 oxidation, and (c) the photocatalytic degradation of C_2H_2 on TiO_2 under plasma exposure. Different glass fibres-based catalytic materials coated with SiO_2 and/or TiO_2 nano-particles are used to separate these three contributions regarding to C_2H_2 conversion. It is reported that at constant voltage the injected power is mainly increased by the presence of glass fibres. C_2H_2 oxidation is mainly enhanced by the macroporosity of glass fibres and in a minor way by the nano-particles. The production of O atoms close to the surface is probably responsible for the higher C_2H_2 removal efficiency with porous material. The photocatalytic activity of TiO_2 is negligible in the plasma except if additional UV lamps are used to activate TiO_2. With external UV, photocatalytic activity is more efficient in the plasma phase than in a neutral gas phase. This plasma/photocatalysis synergy is due to the use of O atoms in photocatalytic mechanisms.
© 2007 Elsevier B.V. All rights reserved.

Keywords: Plasma photocatalysis combination; Dielectric barrier discharge; TiO_2; Porosity; O atoms; C_2H_2 oxidation; Air treatment

1. Introduction

The environmental issue is becoming more and more a world matter of concern. Nowadays many industries need depollution systems at a low energetic cost to be able to respect environmental rules. Non-thermal plasmas have been investigated for pollution control for 30 years. Electron beams [1] and microwave discharges [2] were first studied but corona and dielectric barrier discharges (DBD) are now preferred, especially for volatile organic compounds (VOC) treatment, because of their high reactivity at room temperature. DBD prevent electric arc and treat statistically all the volume of the reactor because the plasma filaments are randomly distributed on the whole dielectric surface by the adsorbed charges. The abatement of many VOCs has already been investigated: alkane (butane [3]), aromatic hydrocarbon (benzene [4], toluene [5]), aldehyde (acetaldehyde [6]), alcohol (phenol [7]), chlorinated compounds (dichloromethane [8]), etc. Nevertheless, plasma generates undesired by-products which may be even more toxic than the initial molecule. Thus, DBD are combined with catalysts to obtain a better control on the chemistry by increasing the oxidation rate with the same energy consumption [9,10].

Several synergetic effects between DBD and catalyst for VOC removal have been reported. The first materials combined with plasma, such as $BaTiO_3$, were often used for their high dielectric permittivity, lowering the discharge breakdown [11]. The activity of noble metal or metal oxide-based catalysts was also investigated [12,13]. The destruction of the initial pollutant occurs with lower energy consumption because no gas heating is required; the oxidation rate and the selectivity into CO_2 are higher with catalyst, and the plasma treatment is expected to prevent catalyst poisoning. Plasma/catalyst combination has definitely positive effects but the mechanisms involved in this synergy have not been deeply investigated.

Ayrault et al. [14] have proved that metallic particles (Pt) have a catalytic activity in the plasma for 2-heptanone conversion by comparing the same support (honeycomb

* Corresponding authors.
E-mail addresses: guaitella@lptp.polytechnique.fr (O. Guaitella), Antoine.rousseau@lptp.polytechnique.fr (A. Rousseau).

0926-3373/$ – see front matter © 2007 Elsevier B.V. All rights reserved.
doi:10.1016/j.apcatb.2007.11.032

monolith) with and without metallic particles. On the other hand, the support itself may have a strong influence on the oxidation because of its porosity. It was shown by Holzer et al. [15] who have compared the effect of SiO_2 and alumina located in the discharge as a function of porosity. In their conditions, they showed that VOC conversion was more influenced by porosity than the chemical nature of the surface. They suggest that O atoms produced by the plasma are used for oxidation, the efficiency of the latter depending on the size of the pores.

Among the catalysts used in DBD, photocatalysts have a very particular chemical activity.

Photocatalysts are semi-conductors activated by photons which create electron–hole pairs, inducing oxidation or reduction reactions at the surface of the material with adsorbed molecules. TiO_2 is one of the most efficient photocatalysts for VOC treatment. The level of the oxidation potential of the valence and conduction bands of TiO_2 is well suited for a wide range of organic compounds [16], and consequently TiO_2 gives a very high selectivity into CO_2 for many pollutants [17,18]. The plasma/TiO_2 combination has been studied since 1999 [19,20] and its benefit was mainly shown on toluene [21,22], benzene [23–27] and a few other molecules [23,28,29,30].

The aim of this work is to distinguish three contributions

(i) The modification of the discharge development itself because of the catalyst.
(ii) The catalyst porosity effect on the chemistry.
(iii) The photocatalytic activity.

The difference between the last two points is the distinction between surface chemical reactions which involve only adsorbed species, and those which involves electron/hole pairs from the catalytic material itself. The three contributions listed above are analyzed by measuring the power injected into the gas with the different catalytic materials (i), comparing the C_2H_2 conversion at constant energy density with or without porous silica materials without any photocatalytic activity (ii), and finally checking the effect of photocatalysis by adding TiO_2 nano-particles without changing the specific area of the porous materials (iii).

2. Experimental setup

2.1. Catalytic materials

The catalytic materials are made of glass fibres coated with nanoscale particles of SiO_2 and/or TiO_2 (Fig. 1). TiO_2 particles of 40 nm (P25 Degussa) cannot be deposited alone on glass fibres (20 μm) and need to be bounded with SiO_2 particles of 20 nm. Materials have been prepared by Ahlstrom research and Services. The coating process consisted in an impregnation of glass fibres using industrial size press.

This material gives the opportunity to change separately either the porosity or the photocatalytic activity of the surface, by changing the nature and the amount of the particles deposited. Four different materials were used for these experiments. The amounts of deposited particles on each

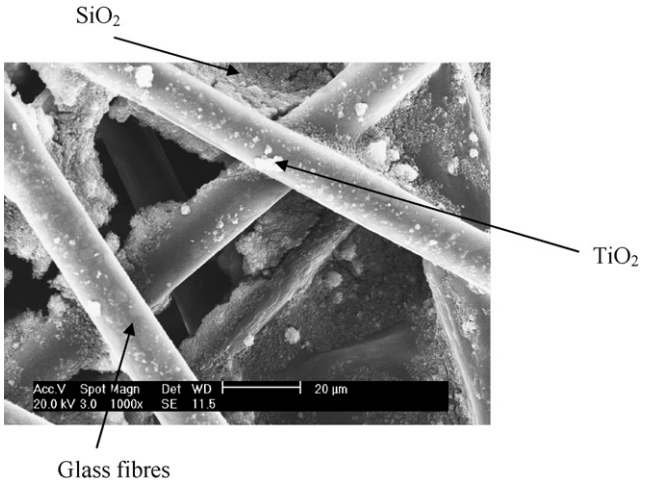

Fig. 1. SEM picture of glass fibres coated with 20 g/m^2 of SiO_2 nano-particles and 20 g/m^2 of TiO_2 nano-particles (material manufactured by Ahlstrom Research and Services).

material are detailed in Table 1. The material called below "fibres", "Si40" and "Si95" have no photocatalytic activity but exhibit different specific areas. "Si40" and "Si20Ti20" have comparable specific areas but only Si20Ti20 has a photocatalytic activity because of TiO_2 nano-particles. In the following, these materials will be referred to as "catalytic materials" but only Si20Ti20 will be called "photocatalyst".

The electrical properties of the discharge and the oxidation of C_2H_2 into CO and CO_2 are measured with a 10 cm long cylinder of one of these materials or without any catalyst, located on the inner surface of the glass tube. The thickness of these materials is less than 100 μm so that the gas gap is not strongly modified by the catalysts.

In order to evaluate microstructural modifications of the titanium dioxide which is used on Si20Ti20, under plasma treatment, two surface analysis techniques have been used to characterize TiO_2 before and after plasma association.

First, X-ray photoelectron spectroscopy has been performed in order to determine titanium atoms valence before and after plasma treatment, as well as relative percentage of the atoms present at TiO_2 surface. No chemical shift has been noticed considering 2p1/2 and 2p3/2 titanium peaks even after a 2 h plasma treatment, thus no valence modification has been evidenced.

Second, Raman spectrometry has been performed in order to evaluate anatase and rutile ratios into titanium dioxide structures, and to check modification of this ratio after plasma exposure. Rutile and anatase allotropic forms have been easily

Table 1
The four catalytic materials used and the amount of SiO_2 and TiO_2 nanoscale particles deposited on each one

Name	Amount of SiO_2 particles (g/m^2)	Amount of TiO_2 particles (g/m^2)	Specific area (BET) (m^2/g)
Fibres	0	0	6
Si20Ti20	20	20	20.6
Si40	40	0	28
Si95	95	0	45

identified and quantified by scaling with synthetic mixtures of anatase and rutile. After a 4 h plasma treatment the ratio of anatase and rutile into titanium dioxide structure is absolutely not modified.

Finally, photocatalytic oxidation of acetylene (with UV lamps irradiation) has been performed with Si20Ti20 before and after ∼50 h of atmospheric DBD air plasma exposure. No modification of the photocatalytic activity is noticed.

Si20Ti20 is then not modified by the plasma used for our experiments.

2.2. Dielectric barrier discharge reactor

The geometry is a classical cylindrical dielectric barrier discharge ignited with a 50 Hz sinusoidal power supply (Fig. 2). Two gas flow controllers enable the regulation of C_2H_2 concentration at 1000 ppm and the total gas flow of dry synthetic air ($H_2O \ll 3$ ppm, Air Liquide) at 500 sccm. Two pressure gauges ensure that the experiment is always performed at 1000 mbar.

The reactor consists in a quartz tube of 15 mm inner diameter and 50 cm long. The dielectric thickness is 1.5 mm. The inner electrode is a threaded rod of 3 mm diameter and the outside ground electrode is a 10 cm long grid. The use of a grid enables to irradiate the catalytic material located inside the discharge with two external UV lamps (Philips PL-L 24W/10/4P) in parallel to the discharge tube. These lamps emit a spectrum band between 350 and 400 nm and the UV intensity induced on the catalytic material is about 5 mW/cm^2. They are placed 5 cm away from the quartz discharge tube in order to make sure that the UV intensity on the material is strong enough to reach saturation of the electron–hole creation rate in TiO_2. Contrary to packed bed reactor, the catalyst is located only on the inner surface of the quartz tube in order to keep the gas gap constant, whether the catalyst is present or not. Thus the discharge is comparable in both conditions contrary to a packed bed reactor which induces surface discharges and cannot be compared to the discharge ignited in an empty tube. The catalytic material used is slim enough to be set onto the inner surface of the tube without changing the gas gap significantly.

2.3. Diagnostics

2.3.1. Manley method

The key parameter to evaluate a depolluting system is the energy consumption. The goal is to perform high pollutant removal with the lowest energetic cost. The most common method used to measure the injected energy into the gas is the Lissajous method (or Manley method [31,32]) which consists in plotting the charges transferred through the gas (Q_{dbd}) versus applied voltage on the DBD reactor (U_{dbd}). This method gives only average data about the discharge.

2.3.2. Chemical diagnostic

A gas chromatograph Varian CP-3800 equipped with a carboBOND column, a methanizer, and a flame ionization detector (FID) was used to measure simultaneously C_2H_2, CO and CO_2. No other by-products were detected in the gas phase. Tests with a CP-sil 5B column using different analysis time and temperature ramps have never shown any other by-products. The sensibility of the gas chromatograph for C_2H_2, CO and CO_2 is about 10 ppm.

Adsorbed carboxylic acids were also analyzed. The catalyst was left under plasma exposure during 30 min for different energy densities, then acids were extracted from the catalytic materials surface with H_2SO_4. The solution was analyzed by high precision liquid chromatography with a sarasep car-H column and a UV detector at 210 nm.

Ozone measurements were performed by broadband UV absorption. A measurement cell was located downstream the reactor. A deuterium lamp (Mikropack DH2000) and a spectrometer (Ocean Optics USB4000) were used to measure the absorption spectrum of O_3 around 250 nm.

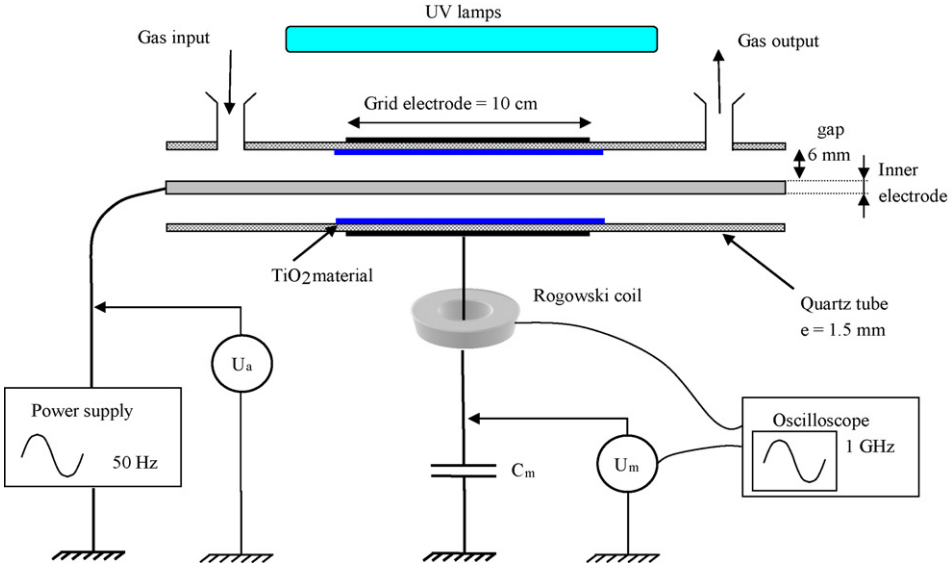

Fig. 2. Experimental setup.

3. Influence of porous material on the injected power

It is well known that catalytic materials located in the discharge could increase the energy injected into the gas for a given applied voltage. For instance, Li et al. have shown that TiO_2 pellets placed between pins to plane electrodes increase the current of the discharge [22]. Most of the time, the comparison is made between empty reactor and packed bed reactor. However, the discharge type is not the same with these two configurations. With empty reactor, plasma filaments cross an empty gas gap. With packed bed reactor, surface discharges are more readily generated on the catalyst pellets because of secondary electron emission from the material itself. For the same applied voltage, the plasma filaments ignited are thus more numerous, and the injected power is higher with packed bed configuration.

In our reactor, the catalytic materials are always onto the inner surface of the tube in order to keep constant the gas gap with or without catalyst.

Fig. 3 shows that for the same applied voltage, the power injected into the gas is increased when catalytic material is added in the plasma zone. This enhancement is exactly the same with Si20Ti20, with Si40, and with fibres; a small additional increase of the power is observed with external UV lamps only with Si20Ti20 in the discharge. The main effect is thus due to the glass fibres. As the catalytic materials is located only onto the surface of the discharge tube, the increase of the injected power is probably a consequence of an easier breakdown of the filaments, and not a consequence of a modification of the propagation mechanism as it could be the case with surface discharges in packed bed reactors. Two main reasons could explain that glass fibres help the filaments breakdown:

- glass fibres are responsible for local electric field enhancement effect because of their small diameter (20 μm),
- the effective surface of the glass fibres is much larger than the surface of the tube so that more charges can be adsorbed on it.

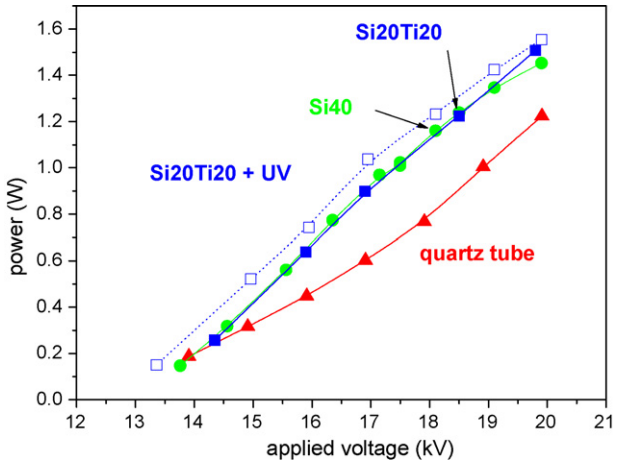

Fig. 3. Power injected into the gas as a function of the voltage applied on the DBD, with or without catalytic material in the discharge. The dotted curve is obtained with external UV lamps.

The second point was studied in detailed in [33]. It has been shown with the same experimental setup that more than the half of the injected power is transferred through less than five large current peaks per period of the power supply, with amplitude of several amperes. These large peaks were attributed to "collective effects" which corresponds to release a great amount of adsorbed charges at the same time, triggered by the light emitted by a first plasma filament. The collective effects are more important with catalytic material because of the greater amount of adsorbed charges on these materials. As a consequence, this explains the higher injected power for a given applied voltage.

The glass fibres have a strong influence on the filaments breakdown in spite of a large gas gap (6 mm). On the contrary, nano-particles of SiO_2 or TiO_2 (respectively 20 and 40 nm in diameter) induce no additional increase of the power. The typical Debye length $\sqrt{\varepsilon_0 kT_e/n_e^2}$ for an electron density n_e equal to 1×10^{14} cm^{-3} and electron energy $T_e = 1$ eV is about 700 nm. This estimation suggests that filaments are not sensitive to geometrical shapes with scale of few tens of nanometres. Consequently the increase of the injected power is mainly driven by the glass fibres and not by the nano-particles. The only additional effect obtained with nano-particles of TiO_2 is observed with external UVs. It could be a consequence of higher secondary electron emission from activated TiO_2 surface, or a continuous desorption of charges stored on the surface as described in [33].

Even with a constant gas gap, the injected power is enhanced by the presence of catalytic material for the same applied voltage, which is an advantage for industrial applications. The chemical efficiency of our plasma/catalyst combination has now to be evaluated for the same injected power.

4. Influence of porous material on C_2H_2 oxidation

4.1. C_2H_2 destruction with or without porous material

Fig. 4 shows the destruction of C_2H_2 as a function of the injected energy density (E_{inj}) for plasma with or without silica

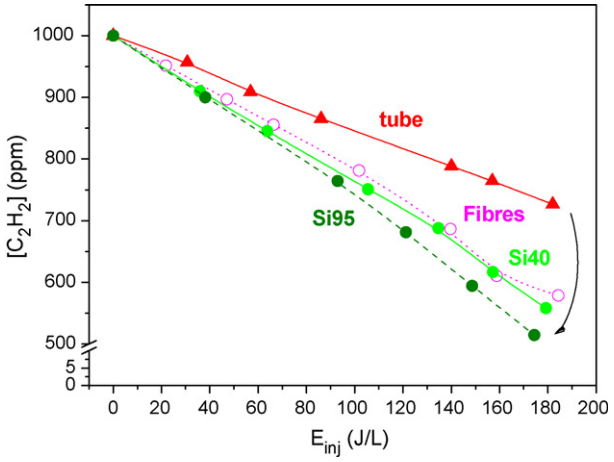

Fig. 4. C_2H_2 concentration as a function of the specific energy with or without porous materials (tube without catalyst in red triangle, fibres in pink dot curve and open circle, Si40 in green filled symbols and Si95 in dark green). (For interpretation of the references to color in this figure legend, the reader is referred to the web version of the article.)

Table 2
C_2H_2 destruction rate measured with the different catalytic materials used

	Effective surface S_{eff} (m)	C_2H_2 destruction rate (ppm L/J)	C_2H_2 destruction rate (mol/J)
Plasma	0.0047	1.51	6.74E−08
Fibres	7.6	2.31	1.03E−07
Si40	35.6	2.42	1.08E−07
Si95	74	2.81	1.25E−07
Si20Ti20	26.4	2.47	1.10E−07
Si20Ti20 + UV	26.4	2.67	1.19E−07

fibres coated with various amounts of silica nano-particles (fibres, Si40 and Si95). These materials have no chemical activity but different specific areas (cf Table 1). C_2H_2 removal is in the range of 1000–500 ppm, always proportional to the injected energy but, as shown in Table 2, the destruction rate increases with the effective surface S_{eff} ($S_{eff} = S_{BET}M$ where M is the weight of material introduced in the discharge in g and S_{BET} is the BET surface in m^2/g). Two main reasons could explain the higher C_2H_2 removal with porous material in the discharge:

(i) a modification of the plasma filaments breakdown and their chemical efficiency due to the catalytic materials;
(ii) the use of species produced by the plasma like O_3, NOx (long life species) or O, O_2* (short live species) for oxidation reactions of C_2H_2 on the surface of the porous materials.

The first point was already mentioned in part 3. Porous material in the discharge could increase the number of collective effect per period. However, we have no evidence for a specific chemical efficiency of collective breakdown compared to successive individual filaments ignition.

In the following parts the role of long life species or short life species is discussed.

4.2. Role of O_3 in surface destruction of C_2H_2

The gas phase reaction rate of O_3 with C_2H_2 at 300 K is very low (1×10^{-20} cm^3/s [34]), so that O_3 is probably not responsible for C_2H_2 destruction in the gas phase. Nevertheless it is well known that O_3 could be dissociated on the surface of different materials like MnO_2 [27] or γ-Al_2O_3 [15], and thus O_3 could increase the efficiency of surface oxidation of many hydrocarbons.

Fig. 5 shows C_2H_2 removal as a function of the specific energy for plasma alone, and plasma with catalytic material located downstream the discharge. The distance between the output of the plasma region and the place where the catalytic material is in the tube is chosen large enough to ensure that the gas need about 2 s to reach the catalyst. As a consequence, only long life species, especially O_3, could reach the catalyst surface.

C_2H_2 removal is not changed at all as the catalyst is located downstream the discharge. This means that long life species and especially O_3 are not able to enhance oxidation of C_2H_2 at the surface of the materials used. This is in good agreement with Holzer et al. who have shown that O_3 is not efficient on silica surface [15] because no surface dissociation was obtained with this material. Therefore, the increase of chemical efficiency obtained with porous material in the plasma region is due to short life species.

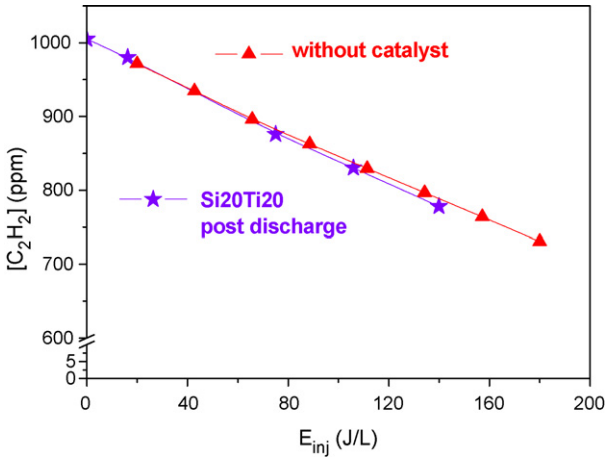

Fig. 5. C_2H_2 removal as a function of the specific energy with the photo-catalytic material (Si20Ti20) located in post-discharge (10 cm after the plasma region, i.e. 2 s after the plasma).

4.3. Role of O atoms in surface destruction of C_2H_2

The direct measurement of O atoms in DBD at atmospheric pressure is a very challenging issue. The measurement of O_3 is an easiest way to get information on O atoms since the main part of O atoms is converted into O_3 in atmospheric air plasma discharge at room temperature.

Fig. 6 shows the production of O_3 in pure air and in air with 1000 ppm of C_2H_2, with or without Si40 in the discharge. Two observations may be exhibited:

(i) the production of O_3 is reduced by a factor of 1.4 when C_2H_2 is added in the gas mixture, with porous material in the discharge as well as without;

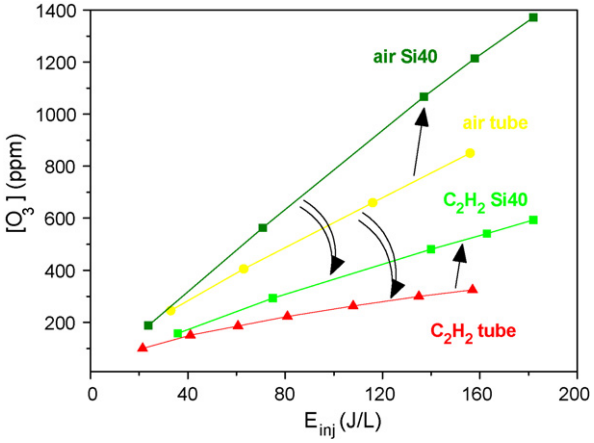

Fig. 6. Production of O_3 in pure air and in air with 1000 ppm of C_2H_2 with or without Si40 as catalytic material. The double arrows show the decrease of O_3 if C_2H_2 is added in the gas mixture, and the single straight arrows show the increase of O_3 with a porous material in the discharge.

(ii) the production of O_3 is enhanced with porous material in the discharge, in pure air as well as in air with C_2H_2.

The lower concentration of O_3 with C_2H_2 is not due to a consumption of O_3 for C_2H_2 oxidation as it was explained in part 4.2. As a consequence, this decrease of O_3 should be due to a consumption of O atoms which reduces the production of O_3. The proportion of O_3 diminution with C_2H_2 admixture is the same with Si40 or without. Moreover this proportion correspond approximately to the number of O atoms necessary to convert all the C_2H_2 destroyed into ~55% of CO and ~45% of CO_2 as it was measured. Thus the oxidizing species involved in the oxidation of C_2H_2 and its by-products seem to be strongly connected with O_3. Therefore, these experimental results suggest that O atoms could be responsible for C_2H_2 oxidation pathway in the gas phase but also on the porous surface. This hypothesis requires that some O atoms reach the surface of porous materials and are then used for oxidizing reactions.

The enhancement of O_3 production with porous silica is another result which suggests an influence of the surface on O atoms production. Jodzis [35] has already reported an influence of porous material located in the discharge on the ozone production and they have attributed this effect to a surface reaction. We suppose that adsorbed O atoms could react with O_2 molecule from the gas phase to produce O_3. The surface of the porous material could play the role of third body and allow better energy dissipation than molecule from the gas phase what could increase the ozone production for the same amount of O atoms produced. Another possible explanation is that more O atoms are produced when porous material is added in the discharge.

For surface oxidation of C_2H_2 and its by-products as well as for O_3 surface production, it seems that O atoms should be produced on or close to the surface of the porous material, or that they can diffuse up to the surface.

4.4. Adsorption of O atoms on porous surface

The diffusion of O atoms at atmospheric pressure limits the amount of O atoms produced in the gas volume which could reach the catalytic material surface. O atoms have a very short life time estimated to 14 μs for O(3P) by Holzer et al. [15] and anyway shorter than 100 μs [36]. The diffusion length is then shorter than 30 μm with a diffusion coefficient of O equal to 0.26 cm^2/s. O atoms produced in the bulk by streamer crossing the 6 mm of gas gap cannot reach the surface. O atoms involved in surface reactions must then be produced close to the surface.

The footprints of streamers could spread over several millimetres on the dielectric surface and could maybe explain an important O atoms production close to the dielectric surface. Besides, Kozlov et al. [37] have measured by cross-correlation spectroscopy that the electric field is in the range of 200–250 Td closed to the dielectric surface instead of ~100 Td in the streamer channel. They have estimated that the maximum of O atoms production is obtained close to the electrode and finally ozone production is two times higher in the 100 μm near the dielectric surface than in the middle of the gas gap.

The favourable electric field condition close to the electrodes and the expansion of filaments on the dielectric are possible explanations to have a large amount of O atoms produced close to the surface and not only in the bulk. A larger amount of O atoms interact with Si40 or fibres than with the tube because of a larger specific area. This was shown with the same materials by measuring the loss probability of O atoms in a pulsed DC discharge at low pressure [38]. However, the specific area is not the only parameter which determines the efficiency of C_2H_2 oxidation by O atoms at the surface and the typical size of the geometry of the surface should be considered too.

4.5. Macro versus mesoporosity

The C_2H_2 destruction rates given in Table 2 in (ppm L/J) are obtained with the slope of the lines from Fig. 4. Fig. 7 plots this destruction rate as a function of the effective surface of the materials inserted in the plasma (S_{eff} as defined in part 4.1). The destruction efficiency always increases with the effective surface but the effect of glass fibres is more significant than the effect of nano-particles deposited on the glass fibres. The ''macroporosity'' due to the glass fibres, seems to be more efficient to enhance the reactivity than the ''mesoporosity'' due to nano-particles of SiO_2 (a structure with pores diameter ranging between 2 and 50 nm is qualified as ''mesoporous'', and ''macroporous'' for pores diameter larger than 50 nm).

The difference between the fibres and the nano-particles for the efficiency of C_2H_2 destruction is probably due to the surface reachable by O atoms because O atoms cannot be produced between nano-particles, and because they cannot either diffuse between nano-particles.

The mean free path of electron in air at atmospheric pressure is in the range of few tens of nanometres. The SiO_2 nano-particles on Si40 and Si95 are aggregated in bundles. The gap length between glass fibres is in the range of few tens of micrometers contrary to the distance between nano-particles

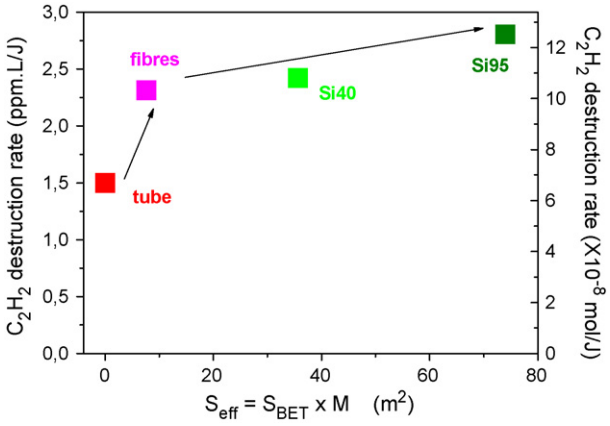

Fig. 7. C_2H_2 removal efficiency plotted as a function of the effective surface S_{eff} inserted into the discharge tube with the different porous materials. The destruction rate is obtained from the slope of linear fits of the results from Fig. 4. The effective surface is obtained by multiplying the specific area measured by BET method (S_{BET}) of each material, by the mass (M) of material used for each experiment.

which is shorter than 50 nm in the bundles which is in the same range as the mean free path of electrons. Even if the reduced electric field in the neighbourhood of surface could reach very high value of several hundred of Townsend when the streamer head meets the dielectric, the voltage applied on a typical distance of less than 10 nm is lower than 0.5 V, what is too low for accelerating electron with the 6 eV required for direct electron impact dissociation of O_2 [39].

The diffusion length of O atoms on SiO_2 nano-particles is difficult to estimate. One of the unknown parameter is how an adsorbed O atom could transit from one nano-particle to another one. Moreover, Holzer et al. have shown that diffusion length of adsorbed O atoms could be reduced by a factor of 1000 if hydrocarbons are also adsorbed on the surface [15]. As a consequence, with C_2H_2 in the gas mixture, it seems likely that O atoms could be adsorbed on particles at the top of bundles but could not diffuse inside the bundles.

These hypotheses may explain that only the envelope of the nano-particles bundles give a contribution to the enhancement of C_2H_2 oxidation by adsorbed O atoms. The higher efficiency of C_2H_2 destruction with porous material is connected with the higher probability for C_2H_2 molecules to meet short live species, especially O atoms. The same effect should increase the oxidation rate and consequently the selectivity into CO_2.

4.6. Comparison of selectivity with and without porous materials

This higher oxidation rate with porous material was already reported by Holzer et al. [15]. However with Si40, glass fibres, or without any materials, the proportions of CO and CO_2 produced from destroyed C_2H_2 remain unchanged in our reactor. Whatever the material used, the carbon balance always exceeds 90% for energy density higher than 60 J/L considering only CO and CO_2. Thus each C_2H_2 molecule seems to be quickly converted into one CO and one CO_2, in gas phase as well as at the surface. Moreover, the conversion of CO into CO_2 required very high energy. With the same experimental setup, when 1000 ppm of CO are introduced with dry air, the conversion into CO_2 as a function of energy density shows that only 100 ppm of CO is converted into CO_2 at 180 J/L. Consequently only minor effect of the porous materials could be obtained on the carbon balance and the selectivity into CO_2 in our conditions.

The macroporosity has the main effect on C_2H_2 oxidation enhancement. If TiO_2 has a real photocatalytic activity which involves electron/hole pairs under plasma exposure, this chemical effect has to be discriminate from the effect of the porosity. The C_2H_2 conversion with Si20Ti20 is thus compared to the conversion with Si40.

5. Plasma/photocatalysis coupling

5.1. Influence of TiO_2 particles on C_2H_2 oxidation by plasma

Si20Ti20 has the same total amount of nano-particles than Si40 (40 g/m^2) but with the ratio $SiO_2/TiO_2 = 50/50$ (see Table 1). Specific areas of Si20Ti20 and Si40 are similar, so that only the chemical nature of the surface is changed, but not its geometry. Fig. 8a–c shows that the conversion of C_2H_2 into CO and CO_2 is exactly the same with Si20Ti20 and Si40. No photocatalytic activity can be distinguished from the effect of the porosity of Si20Ti20 which is comparable to the porosity of

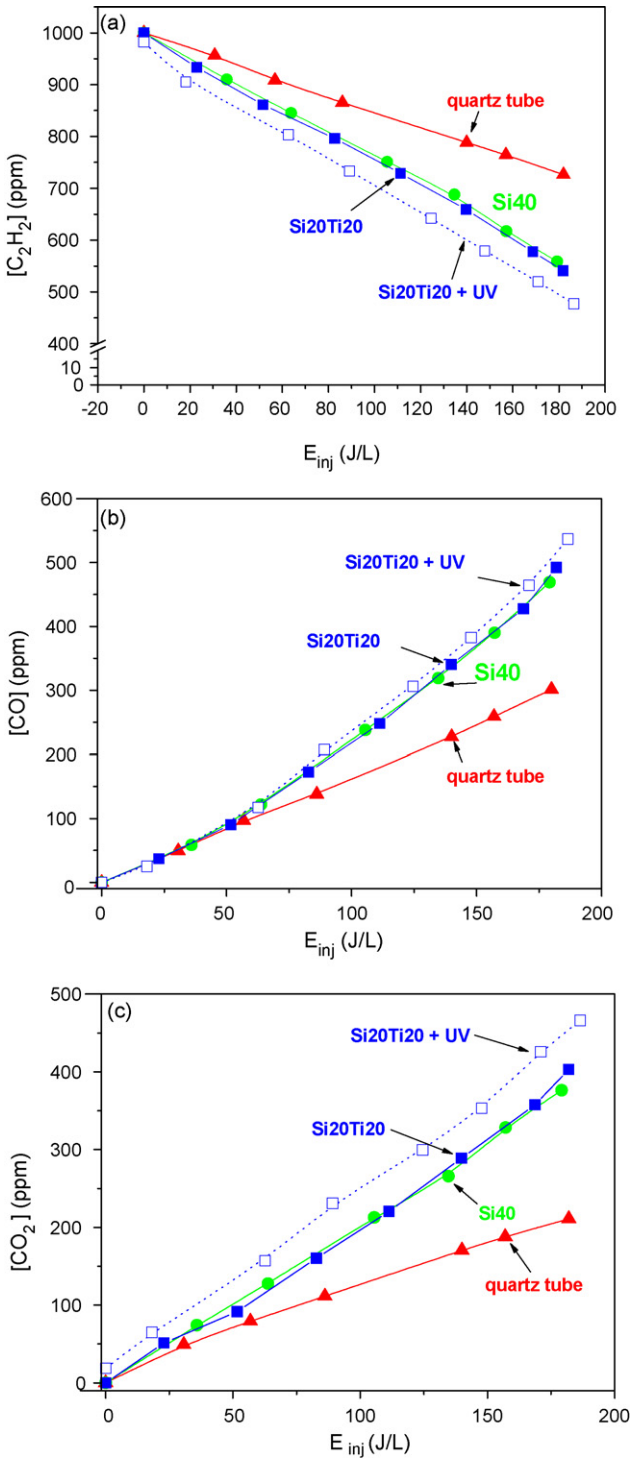

Fig. 8. Comparison of C_2H_2 destruction efficiency (a) and CO (b) and CO_2 (c) production of the DBD without any catalyst, with SiO_2 on glass fibres (Si40) and TiO_2 on glass fibres (Si20Ti20). The dotted curves are obtained with external UV lamps.

Si40. The wide gas gap (6 mm), the short residence time of the gas in the reactor (~2 s) and the small amount of TiO_2 deposited on Si20Ti20 (20 g/m^2) are not favourable to obtain a strong photocatalytic effect in the present experiments. The UV and the ion bombardment from the plasma are not sufficient to activate TiO_2 nano-particles and create enough electron/hole pairs to have a significant contribution on C_2H_2 oxidation. Nevertheless the photocatalytic activity of Si20Ti20 under plasma exposure is investigated in the following by activating TiO_2 with external UV lamps.

5.2. Photocatalysis in plasma induced by external UV irradiation

Dashed curves in Fig. 8a–c are obtained with external UV lamps. The irradiation of Si20Ti20 by external UV lamps allows to be sure that TiO_2 is activated, that means electron–hole pairs are created in the material. Then the efficiency of photocatalytic mechanisms could be evaluated under plasma exposure. Without any material in the discharge, C_2H_2 oxidation is not changed by UV radiations. The photochemistry in the gas bulk can be neglected. The effect of UV with Si20Ti20 is thus connected with surface reactions.

The increase of 10% of C_2H_2 destruction with external UV in presence of TiO_2 (see Table 2) is related to a 20% increase of CO_2, although CO density is unchanged. The high selectivity into CO_2 is a characteristic of photocatalytic oxidation on TiO_2 and was already described for C_2H_2 removal [40]. Besides the same UV irradiation has nearly no effect on Si40. The additional enhancement of C_2H_2 conversion into CO_2 with Si20Ti20 under UV exposure is then a photocatalytic effect. This results means that photocatalysis mechanisms could be efficient under plasma exposure in our reactor but the plasma itself is not able to activate sufficiently TiO_2 nano-particles as it was shown in part 5.1.

Another proof that TiO_2 nano-particles can be involved in photocatalytic mechanisms in the plasma is given by the measurement of carboxylic acids adsorbed on Si20Ti20 and Si40. Seven acids were identified and are detailed in [41]. Fig. 9 shows the part of carbon balance constituted by the total amount of acids detected on the surface of Si40 and Si20Ti20 after 30 min of plasma exposure at 180 J/L with a gas flow of 500 sccm and a C_2H_2 concentration of 1000 ppm. The external UVs have no influence on Si40. Without UV the amount of adsorbed acids is higher on Si20Ti20 than on Si40, and this quantity increases with external UV. This confirms that TiO_2 have a real photocatalytic activity in the plasma phase.

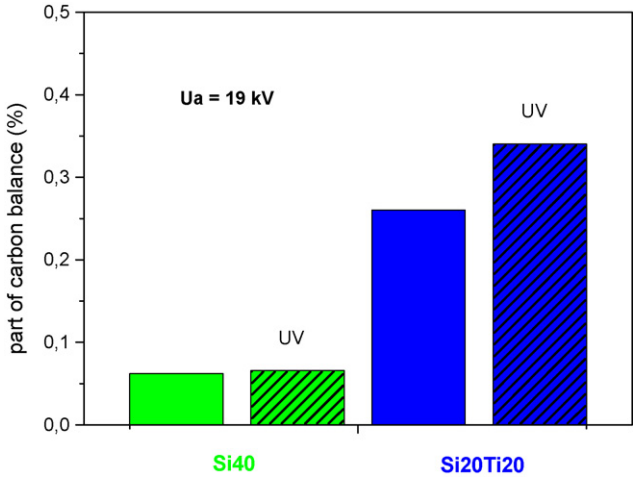

Fig. 9. Amount of carboxylic acids detected on the surface of Si40 and Si20Ti20 after 30 min of plasma exposure at 19 kV (160 J/L) with inlet gas mixture of 1000 ppm of C_2H_2 in dry air.

5.3. Evidence for plasma/TiO_2 synergy

With external lamps under plasma exposure the photocatalytic effect obtained is more important than the simple effect of photocatalysis without plasma. Fig. 10 gives the difference between the amount of C_2H_2 removed by Si20Ti20 with and without UV. This gives an estimation of the contribution of "photocatalysis" in C_2H_2 oxidation under plasma exposure. The same comparison is made for SiO_2 + UV and SiO_2 as well as for plasma + UV and plasma. For SiO_2, a small effect appears and increases with energy but this effect is hardly distinguished from error bars. This could be due to a photo-dissociation of C_2H_2 molecule adsorbed on Si40 surface. The main effect is a clear increase of photocatalytic destruction of C_2H_2 on Si20Ti20 with the injected energy.

"Photocatalysis" without plasma in our reactor (i.e. Si20Ti20 under external UV lamps exposure) is able to destroy 18 ppm of C_2H_2 (pink circle at energy equal to 0 in Fig. 10). This value is in good agreement with the destruction rate obtained by Thevenet et al. with the same material [40] by taking into account the surface of Si20Ti20 used and the volume of gas treated by unit of time (about 0.3 mmol cm^{-2} s^{-1}). The photocatalytic efficiency is enhanced under plasma exposure, and increases with the injected energy. Such a synergetic effect between plasma and TiO_2 has been also recently evidenced in a pulsed low pressure DC discharge by IR absorption spectroscopy [42].

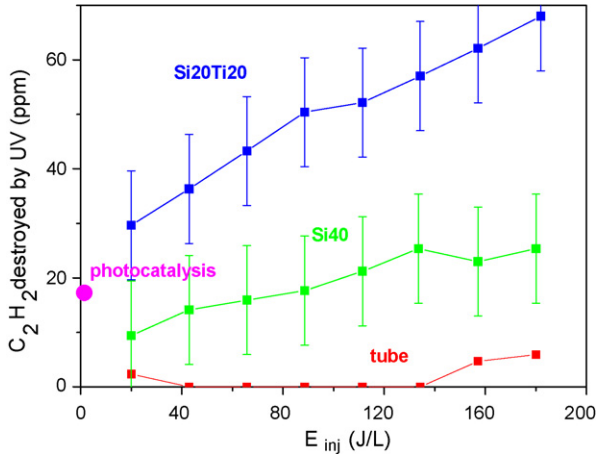

Fig. 10. Estimation of the photocatalytic activity of TiO_2 in the plasma obtained from the difference between the curves of Fig. 8a with and without UV made for the same energy density. The pink point named "photocatalysis" is the amount of C_2H_2 destroyed without plasma by Si20Ti20 in the same reactor irradiated by the UV lamps. (For interpretation of the references to color in this figure legend, the reader is referred to the web version of the article.)

The enhancement of photocatalysis under plasma exposure may be due to a better turn over of adsorbed oxidizing species because of the ion bombardment. However, this effect could not be proved at this time at atmospheric pressure. Another explanation is the use of oxidizing species produced by plasma in photocatalytic mechanisms.

5.4. Role of O and O_3 in photocatalysis under plasma exposure

The use of ozone in photocatalytic process was already described in the literature. Ohtani et al. [43] have shown that photocatalysis aided by ozone is more efficient because O_3 can be decomposed on activated TiO_2. However, in our reactor no improvement of C_2H_2 destruction was obtained with Si20Ti20 located downstream the discharge. Only a small increase of CO_2 production is measured when external UV lamps are switched on showing that O_3 is involved in photocatalytic oxidation of C_2H_2 by-products adsorbed on Si20Ti20 but not directly in C_2H_2 destruction. The photocatalytic enhancement of C_2H_2 oxidation is obtained only if Si20Ti20 is located in the discharge. Short life species from the plasma are then involved in C_2H_2 oxidation by photocatalytic processes.

It is likely that O atoms are involved in photocatalysis coupled with plasma because of the special behaviour of O atoms on TiO_2 nano-particles. It has been recently shown in low pressure pulsed DC discharge in pure air that O atoms kinetics during a series of plasma pulses is different with Si20Ti20 than with Si40. The measured density of O atoms shows a two slope decay between plasma pulses and a desorption peak at the beginning of plasma pulse only with TiO_2 nano-particles. These observations point out that O atoms could be adsorbed without being recombined on TiO_2 nano-particles during long time (>1 s at 1.6 Torr). These O atoms available on TiO_2 surface could be responsible for the enhancement of photocatalysis under plasma exposure.

5.5. Contributions to C_2H_2 destruction in our plasma/photocatalysis coupling system

It has been proven that synergetic effect between plasma and photocatalytic reactions with electron/holes pairs exists but is not the main effect with our geometry. The plasma itself and the influence of the effective surface of the material are more important in our conditions for the C_2H_2 destruction. Fig. 11 shows that C_2H_2 destruction is nearly proportional to the energy density in the energy range used. By considering the differences between the slopes of the curve obtained with plasma only system (p), plasma with Si20Ti20 (p + Ti), and plasma with Si20Ti20 and external UV (p + Ti + UV), the proportion of the contribution due to the plasma, the effective surface, and the photocatalytic activity could be estimated. The difference (p + Ti + UV)-(p) shows that 53% of the total amount of C_2H_2 destroyed in our plasma/photocatalysis coupling system, is probably destroyed simply by the gas bulk chemistry of the plasma (see Fig. 11). The difference (p + Ti)-(p) gives an estimation of the influence of the effective surface of the dielectric because the slope (p + Ti) is nearly the same as the slope obtained with Si40 in the discharge instead of Si20Ti20. By doing this, the influence of effective surface is about 33% of what is destroyed in (plasma + Si20Ti20 + UV) system. The geometry of the surface is then a very important parameter despite the large gas gap used for these experiments (6 mm). Finally, the difference (p + Ti + UV)-(p + Ti) shows that only 14% of C_2H_2 destruction is due to photocatalytic mechanisms in our conditions. This proportion has to be enhanced to really have the benefit of photocatalysis in term of selectivity for instance.

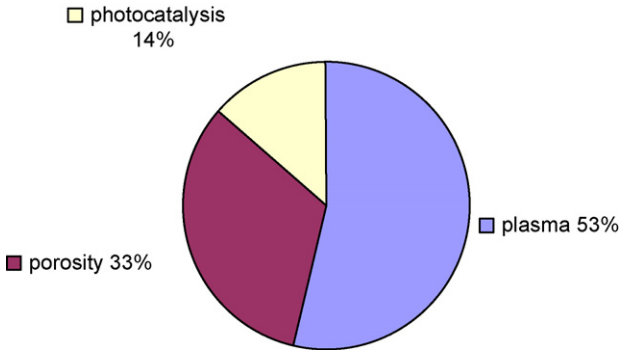

Fig. 11. Proportion of the different contributions involved in C_2H_2 destruction in plasma/TiO_2 combination calculated from the slope of the linear fit from curves of Fig. 8a. The plasma contribution is the ratio between slope obtained for plasma alone and slope obtained for plasma with Si20Ti20 and external UV. The porosity contribution is estimated from the difference between curve for Si20Ti20 without UV (similar to curve for Si40) and curve for plasma alone. The photocatalysis contribution is estimated from the difference between Si20Ti20 with UV and Si20Ti20 without UV.

6. Conclusions

Coupling a TiO_2-based photocatalyst with a non-thermal plasma induces several synergetic effects which are not all connected with photocatalytic mechanisms. At least four effects have to be distinguished to have a clear understanding of plasma/TiO_2 synergy:

- Catalytic material with TiO_2 increases the injected energy for the same applied voltage because of an easier breakdown of the filaments probably due to a larger amount of adsorbed charges and a higher local electric field with the high permittivity of TiO_2 (Fig. 3).
- For the same injected energy, TiO_2 may change the breakdown mechanisms of filaments [33].
- The porosity of the catalytic material increases the efficiency of reactions induced by the species produced by the plasma, probably because of a better contact between reagents when they are adsorbed.
- An improved photocatalytic reactivity involving electron–hole pairs of TiO_2 may occur in contact with plasma phase, if TiO_2 is sufficiently activated.

In our experimental setup, UV and energetic particles produced by the plasma are not sufficient to activate TiO_2 nano-

particles. Nevertheless, with external UV lamps there is evidence for plasma/photocatalysis synergy. Photocatalytic reactions exist and are more efficient in the plasma phase than in neutral gas phase. This synergetic effect is probably due to the use of plasma-generated radicals and ozone by activated TiO_2.

From the applications point of view, it should be very important to find ways to reinforce the proportion of photocatalysis in the VOC removal by plasma/TiO_2 combination because photocatalysis increases significantly the selectivity into CO_2 even in the plasma phase. A better contact between the catalyst and the gas phase may increase this proportion but the issue is to find a way to activate TiO_2 sufficiently to have the benefit of plasma enhanced photocatalysis.

Acknowledgments

The authors want to thank the French Agency for Environment and Energy Saving (ADEME), CIAT and Ahlstrom Research and Services for their financial and technical support.

References

[1] B. Penetrante, M. Hsiao, B.T. Meritt, G.E. Voglin, P.H. Wallman, IEEE Trans. Plasma Sci. 23 (1996) 679.
[2] M. Baeva, H. Gier, A. Pott, J. Uhlenbusch, J. Ḧoschele, J. Steinwandel, Plasma Sources Sci. Technol. 11 (2002) 1–9.
[3] S. Futamura, A. Zhang, G. Prieto, T. Yamamoto, IEEE Trans. Ind. Appl. 34 (1998) 967.
[4] A. Ogata, D. Ito, K. Mizuno, S. Kushiyama, A. Gal, T. Yamamoto, Appl. Catal. A: Gen. 236 (2002) 9.
[5] S. Delagrange, L. Pinard, J.M. Tatibouet, Appl. Catal. B: Environ. 68 (2006) 92.
[6] H.M. Lee, M.B. Chang, Plasma Chem. Plasma Process. 21 (2001) 329.
[7] U. Roland, F. Holzer, F.-D. Kopinke, Catal. Today 73 (2002) 315.
[8] C. Fitzsimmons, F. Ismail, J.C. Whitehead, J.J. Wilman, J. Phys. Chem. A 104 (2000) 6032.
[9] J.-S. Chang, P.A. Lawless, T. Yamamoto, IEEE Trans. Plasma Sci. 19 (1991) 1102–1166.
[10] S. Pasquiers, Eur. Phys. J. Appl. Phys. 28 (2004) 319.
[11] T. Yamamoto, K. Ramanathan, P.A. Lawless, D.S. Ensor, J.R. Newsom, G.H. Ramsey, IEEE Trans. Ind. Appl. 28 (1992) 528.
[12] T. Yamamoto, P.A. Lawless, M.K. Owen, D.S. Ensor, C. Boss, Non-Thermal Plasma Techniques for Pollution Control NATO ASI Series, vol. 34, Springer, Berlin, 1993.
[13] C.M. Nunez, G.H. Ramsey, W.H. Ponder, J.H. Abbott, L.E. Mammel, P.H. Kariher, Air Waste 43 (1993) 242.
[14] C. Ayrault, J. Barrault, N. Blin-Simiand, F. Jorand, S. Pasquiers, A. Rousseau, J.M. Tatibouët, Catal. Today 89 (2004) 75–81.
[15] F. Holzer, U. Roland, F.-D. Kopinke, Appl. Catal. B: Environ. 38 (2002) 163–181.
[16] M. Miyauchi, A. Nakajima, T. Watanabe, K. Hashimoto, Chem. Mater. 14 (2002) 2812.
[17] O. Carp, C.L. Huisman, A. Reller, Prog. Solid State Chem. 32 (2004) 33–177.
[18] U. Diebold, Surf. Sci. Rep. 48 (2003) 53.
[19] A. Mizuno, Y. Kisunaki, M. Nogushi, S. Katsura, S.-H. Lee, Y.-K. Hong, S.-Y. Shin, J.-H. Kang, IEEE Trans. Ind. Appl. 35 (1999) 1284.
[20] T. Oda, T. Takahashi, S. Kohzuma, Conference Records of the IEEE/IAS Annual Meeting, 1999, p. 1489.
[21] M. Kang, B.-J. Kim, S.M. Cho, C.-H. Chung, B.-W. Kim, G.Y. Han, K.J. Yoon, J. Mol. Catal. A: Chem. 180 (2002) 125–132.
[22] D. Li, D. Yakushiji, S. Kanazawa, T. Ohkubo, Y. Nomoto, J. Electrostat. 55 (2002) 311–319.
[23] C.H. Ao, S.C. Lee, Appl. Catal. B: Environ. 44 (2003) 191.
[24] H.-H. Kim, Y.-H. Lee, A. Ogata, S. Futamura, Catal. Commun. 4 (2003) 347–351.
[25] H.-H. Kim, A. Ogata, S. Futamura, J. Korean Phys. Soc. 44 (5) (2004) 1163–1167.
[26] B.-Y. Lee, S.-H. Park, S.-C. Lee, M. Kang, S.-J. Choung, Catal. Today 93 (2004) 769–776.
[27] S. Futamura, H. Einaga, H. Kabashima, L.Y. Hwan, Catal. Today 89 (2004) 89–95.
[28] H.H. Kim, K. Takashima, S. Katsura, A. Mizuno, J. Phys. D: Appl. Phys. 34 (2001) 604–613.
[29] H.H. Kim, S.M. Oh, A. Ogata, S. Futamura, Appl. Catal. B: Environ. 56 (2005) 213.
[30] C.H. Ao, S.C. Lee, Chem. Eng. Sci. 60 (2005) 103.
[31] T.C. Manley, Trans. Electrochem. Soc. 84 (1943) 83–96.
[32] Z. Falkenstein, J.J. Coogan, J. Phys. D: Appl. Phys. 30 (1997) 817–825.
[33] O. Guaitella, F. Thevenet, C. Guillard, A. Rousseau, J. Phys. D: Appl. Phys. 39 (2006) 2964.
[34] R. Atkinson, D.L. Baulch, R.A. Cox, J.N. Crowley, R.F. Hampson, J.A. Kerr, M.J. Rossi, J. Troe, J. Phys. Chem. Ref. Data 26 (1997) 521–1011.
[35] S. Jodzis, Ozone Science and Engineering, Taylor & Francis, 2003.
[36] B. Eliason, U. Kogelschatz, IEEE Trans. Plasma Sci. 19 (1991) 1063.
[37] K.V. Kozlov, H.-E. Wagner, R. Brandenburg, P. Michel, J. Phys. D: Appl. Phys. 34 (2001) 3164–3176.
[38] K. Allegraud, O. Guaitella, L. Gatilova, A. Rousseau, Proceeding of 18th International Symposium on Plasma Chemistry, Kyoto, (2007), pp. 17P–28P.
[39] B. Eliasson, U. Kogelschatz, J. Phys. B: Atom. Mol. Phys. 19 (1986) 1241–1247.
[40] F. Thevenet, O. Guaitella, J.M. Herrmann, A. Rousseau, C. Guillard, Appl. Catal. B: Environ. 61 (2005) 62–72.
[41] F. Thevenet, O. Guaitella, E. Puzenat, J.-M. Herrmann, A. Rousseau, C. Guillard, Catal. Today 122 (2007) 186–194.
[42] A. Rousseau, O. Guaitella, L.V. Gatilova, C. Guillard, F. Thevenet, J. Roepcke, G. Stancu, Appl. Phys. Lett. 87 (2005) 221501.
[43] B. Ohtani, S.-W. Zhang, T. Ogita, S. Nishimoto, T. Kagiya, J. Photochem. Photobiol. A: Chem. 71 (1993) 195.